Two [Fe(IV)O Trp •] Intermediates in M. tuberculosis Catalase−Peroxidase Discriminated by Multifrequency (9−285 GHz) EPR Spectroscopy: Reactivity toward Isoniazid

ARTICLE *in* JOURNAL OF THE AMERICAN CHEMICAL SOCIETY · JANUARY 2008

Impact Factor: 12.11 · DOI: 10.1021/ja075108u · Source: PubMed

4 AUTHORS, INCLUDING:

Rahul Singh
University of British Columbia - Vancouver
19 PUBLICATIONS **610** CITATIONS

J|A|C|S
ARTICLES
Published on Web 12/04/2007

Two [Fe(IV)=O Trp•] Intermediates in *M. tuberculosis* Catalase-Peroxidase Discriminated by Multifrequency (9−285 GHz) EPR Spectroscopy: Reactivity toward Isoniazid

Rahul Singh,[†] Jack Switala,[‡] Peter C. Loewen,[‡] and Anabella Ivancich*,[†]

Contribution from the Service de Bioénergétique, Biologie Structurale et Mécanismes, URA 2096 CNRS and iBiTec-S, CEA Saclay, 91191 Gif-sur-Yvette, France and Department of Microbiology, University of Manitoba, Winnipeg, Canada R3T 2N2

Received July 10, 2007; E-mail: anabella.ivancich@cea.fr

Abstract: We have characterized the intermediates formed in the peroxidase cycle of the multifunctional heme-containing enzyme KatG of *M. tuberculosis*. Selected Trp variants from the heme proximal (W321F) and distal (W107F and W91F) sides were analyzed together with the wild-type enzyme with regard to the reaction with peroxyacetic acid and hydrogen peroxide (in the catalase-inactive W107F). The 9 GHz EPR spectrum of the enzyme upon reaction with peroxyacetic acid showed the contribution of three protein-based radical species, two Trp• and a Tyr•, which could be discerned using a combined approach of multifrequency Electron Paramagnetic Resonance (EPR) spectroscopy with selective deuterium labeling of tryptophan and tyrosine residues and site-directed mutagenesis. Trp321, a residue in H-bonding interactions with the iron through Asp381 and the heme axial ligand His270, was identified as one of the radical sites. The 9 GHz EPR signal of the Trp321 radical species was consistent with an exchange-coupled species similar to the oxoferryl−Trp radical intermediate in cytochrome *c* peroxidase. On the basis of the possibility of distinguishing among the different radical intermediates of the peroxidase cycle in *M. tuberculosis* KatG (MtKatG), we used EPR spectroscopy to monitor the reactivity of the enzyme and its W321F variant with isoniazid, the front-line drug used in the treatment of tuberculosis. The EPR experiments on the W321F variant preincubated with isoniazid allowed us to detect the short-lived [Fe(IV)=O Por•+] intermediate. Our results showed that neither the [Fe(IV)=O Por•+] nor the [Fe(IV)=O Trp_{321}•+] intermediates were the reactive species with isoniazid. Accordingly, the subsequent intermediate (most probably the other Trp•) is proposed to be the oxidizing species. Our findings demonstrate that the protein-based radicals formed as alternative intermediates to the [Fe(IV)=O Por•+] can play the role of cofactors for substrate oxidation in the peroxidase cyle of KatGs.

Introduction

In the past years considerable attention has been given to the biochemical, biophysical, and structural characterization of the heme-containing catalase-peroxidase encoded by the *katG* gene in *Mycobacterium tuberculosis* (MtKatG). Specific interest in this enzyme has been triggered by the demonstration that mutations or deletion of the *katG* gene from *M. tuberculosis* were associated with resistance to the prodrug isoniazid (INH) detected in clinical isolates.[1] Isonicotinic acid hydrazide (isoniazid) has served as the core of the chemotherapy used for the treatment of tuberculosis for more than 50 years. The INH mechanism of action involves an indirect role in compromising the integrity of the mycobacteria cell wall through inhibition of the mycolic acid biosynthesis.[2] The primary step of the inhibition is inactivation[3] of the NADH-specific enoyl reductase[4] (InhA) by the isonicotinoyl−NAD adduct. Formation of the adduct between INH and NAD^+ implies the involvement of a radical reaction possibly catalyzed by MtKatG. The mechanistic details of this reaction are not well understood despite the availability of the crystal structures for the KatG enzymes from *M. tuberculosis*,[5] *H. marismortui*,[6] *B. pseudomallei*,[7] and *Synechococcus* PCC7492.[8] On the basis of comprehensive kinetic studies of wild-type MtKatG and key mutations that modify the enzyme activity, putative intermediates of the

[†] Service de Bioénergétique, Biologie Structurale et Mécanismes.
[‡] University of Manitoba.

(1) Zhang, Y.; Heym, B.; Allen, B.; Young, D.; Cole, S. *Nature* **1992**, *358*, 591−593.
(2) Daniel, T. M.; Bates, J. H.; Downes, K. A. In *Tuberculosis Pathogenesis, Protection and Control*; Bloom, B. R., Ed.; American Society for Microbiology Press: Washington, DC, 1999; pp 13−24.
(3) Johnsson, K.; King, D. S.; Schultz, P. G *J. Am. Chem. Soc.* **1995**, *117*, 5009−5010.
(4) Dessen, A.; Quemard, A., Blanchard, J. S.; Jacobs, W. R.; Sacchettini, J. C. *Science* **1995**, *267*, 163 8−1641.
(5) (a) Bertrand, T.; Eady, N. A.; Jones, J. N.; Jesmin; Nagy, J. M.; Jamart-Gregoire, B.; Raven, E. L.; Brown, K. A. *J. Biol. Chem.* **2004**, *279*, 38991−9.
(6) Yamada, Y.; Fujiwara, T.; Sato, T.; Igarashi, N.; Tanaka, N. *Nat. Struct. Biol.* **2002**, *9*, 691−695.
(7) (a) Carpena, X.; Loprasert, S.; Mongkolsuk, S.; Switala, J.; Loewen, P. C.; Fita, I. *J. Mol. Biol.* **2003**, *327*, 475−489. (b) Deemagarn, T.; Wiseman, B.; Carpena, X.; Ivancich, A.; Fita, I.; Loewen, P. C. *Proteins* **2007**, *66*, 219−228.
(8) Wada, K.; Tada, T.; Nakamura, Y.; Kinoshita, T.; Tamoi, M.; Sigeoka, S.; Nishimura, K. *Acta Crystallogr*. **2002**, *D58*, 157−159.

10.1021/ja075108u CCC: $37.00

peroxidase cycle have been proposed[9−12] together with the possible pathways for the enzyme reaction with isoniazid and formation of the isonicotinoyl−NAD adduct either through the peroxidase reaction[13,14] or by means of the oxyferrous state of MtKatG, resulting from the ferric enzyme reaction with superoxide.[15,16] It was also shown that *B. pseudomallei* KatG (BpKatG) can catalyze formation of isonicotinoyl−NAD directly from INH and NAD^+ independent of any added oxidant,[17,18] suggesting an enzyme reaction pathway clearly different from the peroxidase reaction.

In monofunctional heme peroxidases, the main oxidizing species is the porphyrin-based radical intermediate known as Compound I, consisting of an oxoferryl moiety and a porphyrin cation radical [Fe(IV)═O $Por^{\bullet+}$]. In particular cases an alternative intermediate with the radical formed by intramolecular electron transfer between the porphyrin and a defined amino acid residue has been shown to be the oxidizing species for reaction with specific substrates. Specifically, the [Fe(IV)═O $Trp^{\bullet+}$] intermediate formed subsequently to the [Fe(IV)═O $Por^{\bullet+}$] species reacts with cytochrome *c* in cytochrome *c* peroxidase[19] (CcP) and with veratryl alcohol in ligin peroxidase.[20] Interestingly, both substrates bind at the enzyme surface but the Trp radical sites are different. In the case of MtKatG, the studies by Magliozzo and co-workers showed no EPR signal consistent with the [Fe(IV)═O $Por^{\bullet+}$] even when the intermediates were trapped in the milliseconds time scale by the rapid-mix freeze−quench technique. A tyrosyl radical species formed on Tyr353 (a Tyr that is not conserved in other KatG enzymes) was proposed to be the radical site.[21] Very recently, a revised interpretation of the 9 GHz EPR data together with the 130 GHz EPR spectrum of the radical intermediates led the authors to propose formation of $Trp^{\bullet}$ as a minority species.[22] We have previously shown that in *Synechocystis* KatG (SyKatG), the [Fe(IV)═O $Por^{\bullet+}$] intermediate and two subsequent protein-based radical species, $Trp^{\bullet}$ and $Tyr^{\bullet}$, were discerned by their distinct EPR signal contributing to the 9 and 285 GHz EPR spectrum.[23] Trp106, a residue that belongs to a KatG-specific short loop close to the enzyme surface, was shown to be the unique site for the Trp radical formation in SyKatG.[24]

As part of a more general investigation of the radical intermediates formed by selected representatives of the catalase-peroxidase family, we investigated the MtKatG enzyme using multifrequency (9−285 GHz) EPR spectroscopy combined with deuterium labeling of Trp and Tyr residues on the wild-type enzyme and selected Trp variants. The specific aim was to determine if the apparent differences reported so far on the *Synechocystis* and *M. tuberculosis* KatGs with regard the chemical nature of the intermediates, yields, and radical sites could be related to the different reactivity of the enzymes with INH. Our studies show that a short-lived [Fe(IV)═O $Por^{\bullet+}$], two $Trp^{\bullet}$, and a $Tyr^{\bullet}$ are formed in MtKatG. One of the radical sites is identified as the proximal Trp (Trp321; the same site as in cytochrome *c* peroxidase), while the other $Trp^{\bullet}$ appeared to be formed on a different site than that of *Synechocystis* KatG. The reactivity of the Trp radical intermediates with INH was also carefully monitored by EPR spectroscopy.

Materials and Methods

Samples Preparation. *Strains and Plasmids.* The plasmid pAH1[25] was used as a source for catalase peroxidase from *M. tuberculosis*. The plasmid was transformed into strain UM262 *pro leu rpsL hsdM hsdR endI lacY katG2 katE12*::Tn*10 recA* for expression and isolation of the wild-type and variant KatG proteins.[26] Phagemids pKS^+ and pKS^- from Stratagene Cloning Systems were used for mutagenesis, sequencing, and cloning. *E. coli* strains NM522 (*supE thi*)(*lac-proAB*) *hsd-5* [F' *proAB lacI*^{q} *lacZ*)*15*],[27] JM109 (*recA1 supE44 endA1 hsdR17 gyrA96 relA1 thi) (lac-proAB*),[28] and CJ236 (*dut-1 ung-1 thi-1 relA1*/ pCJ105 F′)[29] were used as hosts for the plasmids and generation of single-stranded phage DNA using helper phage R408.

Mutagenesis. The oligonucleotides GAGGTCGTA**TTC**ACGAACACC (TTC encoding Phe in place of Trp 321), CAGCCGTGG**TTC**CCCGCCGAC (TTC encoding Phe in place of Trp 91), and GGCAGCGTGG**AA**CGCCATCCGGAT (GGA from the complementary strand encoding Phe in place of Trp 107) were purchased from Invitrogen. They were used to mutagenize 500 bp fragments from pAH1 generated by *Cla*I-*Xho*I and *Eco*RV-*Cla*I restriction following the Kunkel procedure,[29] which were subsequently reincorporated into pAH1 to generate the mutagenized *katG* gene. Sequence confirmation of all sequences was done by the Sanger method[30] on double-stranded plasmid DNA generated in JM109. The plasmids were transformed into the KatG-deficient *E. coli* strain UM262 (*pro leu rpsL hsdM hsdR endI lacY katE1 katG17*::Tn10 *recA*)[31] and grown in Luria broth containing 10 g/L tryptone, 5 g/L yeast extract, and 5 g/L NaCl for expression of the KatG. Subsequent purification of the enzymes was as described.[32] Hemin chloride (40 mg L^{-1}) was exogenously added to the growth medium to improve incorporation of heme.

Isotope Labeling. Attempts to grow UM262 transformed with pAH1 in minimal medium for incorporation of perdeuterated tryptophan or tyrosine resulted in poor yields of KatG coupled with less than 20% incorporation of the perdeuterated amino acids. To overcome this problem *M. tuberculosis katG* and the variant genes were cloned into pET28b+ vector on a *Eco*RI/*Hin*dIII fragment generated by PCR

(9) Chouchane, S.; Girotto, S.; Yu, S.; Magliozzo, R. S. *J. Biol. Chem.* **2002**, *277*, 42633−42638.
(10) Yu, S.; Chouchane, S.; Magliozzo, R. S. *Protein Sci.* **2002**, *11*, 58−64.
(11) Yu, S.; Girotto, S.; Lee, C.; Magliozzo, R. S. *J. Biol. Chem.* **2003**, *278*, 14769−14775.
(12) Kapetanaki, S. M.; Chouchane, S.; Yu, S.; Magliozzo, R. S.; Schelvis, J. P. *J. Inorg. Biochem.* **2005**, *99*, 1401−1406.
(13) Zhao, X.; Yu, H.; Yu, S.; Wang, F.; Sacchettini, J. C.; Magliozzo, R. S. *Biochemistry* **2006**, *45*, 4131−4140.
(14) Ghiladi, R. A.; Medzihradszky, K. F.; Rusnak, F. M.; Ortiz de Montellano, P. R. *J. Am. Chem. Soc.* **2005**, *127*, 13428−13442.
(15) Wengenack, N. L.; Hoard, H. M.; Rusnak, F. *J. Am. Chem. Soc.* **1999**, *121*, 9748−9749.
(16) Ghiladi, R. A.; Cabelli, D. E.; Ortiz de Montellano, P. R. *J. Am. Chem. Soc.* **2004**, *126*, 4772−4773.
(17) Deemagarn, T.; Carpena, X.; Singh, R.; Wiseman, B.; Fita, I.; Loewen, P. C. *J. Mol. Biol* **2005**, *345*, 21−28.
(18) Singh, R.; Wiseman, B.; Deemagarn, T.; Donald, L. J.; Duckworth, H. W.; Carpena, X.; Fita, I.; Loewen, P. C. *J. Biol. Chem.* **2004**, *279*, 43098−43106.
(19) Sivaraja, M.; Goodin, D. B.; Smith, M.; Hoffman, B. M. *Science* **1989**, *245*, 738−740.
(20) Doyle, W. A.; Blodig, W.; Veitch, N. C.; Piontek, K.; Smith, A. T. *Biochemistry* **1998**, *37*, 15097−15105.
(21) Zhao, X.; Girotto, S.; Yu, S.; Magliozzo, R. S. *J. Biol. Chem.* **2004**, *279*, 7606−7612.
(22) Ranguelova, K.; Girotto, S.; Gerfen, G. J.; Yu, S.; Suarez, J.; Metlitsky, L.; Magliozzo, R. S. *J. Biol. Chem.* **2007**, *282*, 6255−6264.
(23) Ivancich, A.; Jakopitsch, C.; Auer, M.; Un, S.; Obinger, C. *J. Am. Chem. Soc.* **2003**, *125*, 14093−14102.
(24) Jakopitsch, C.; Obinger, C.; Un, S.; Ivancich, A. *J. Inorg. Biochem.* **2006**, *100*, 1091−1099.
(25) Hillar, A.; Loewen, P. C. *Arch. Biochem. Biophys.* **1995**, *323*, 438−446.
(26) Triggs-Raine, B. L.; Loewen, P. C. *Gene* **1987**, *52*, 121−128.
(27) Mead, D. A.; Skorupa, E. S.; Kemper, B. *Nucleic Acids Res.* **1985**, *13*, 1103−1118.
(28) Yanisch-Perron, C.; Vieira, J.; Messing, J. *Gene* **1985**, *33*, 103−119.
(29) Kunkel, T. A.; Roberts, J. D.; Zakour, R. A. *Methods Enzymol.* **1987**, *154*, 367−82.
(30) Sanger, F.; Nicklen, S.; Coulson, A. R. *Biotechnology* **1992**, *24*, 104−108.
(31) Loewen, P. C.; Switala, J.; Smolenski, M.; Triggs-Raine, B. L. *Biochem. Cell Biol.* **1990**, *68*, 1037−1044.
(32) Donald, L. J.; Krokhin, O. V.; Duckworth, H. W.; Wiseman, B.; Deemagarn, T.; Singh, R.; Switala, J.; Carpena, X.; Fita, I.; Loewen, P. C. *J. Biol. Chem.* **2003**, *278*, 35687−35692.

amplification of the genes using the primers AACACCCACC**GAATTC**AGAAACCAC (encoding an EcoRI site) and CGACTAA**TTCGAA**CTAGCC (encoding a *Hin*dIII site). The plasmids were transformed into *E. coli* BL21trxB (DE3) [pLysS F^- *ompT* $hsdS_b(r_b^- m_b^-)$ *gal dcm trxB*15::kan (DE3) pLys(Cm^R)] cells (Novagen). The cells were grown in minimal medium for 3 h before addition of isopropyl α-thiogalactoside (IPTG) to induce expression. Perdeuterated amino acids (CDN Isotopes) were added to the growth medium 30 min prior to induction for best incorporation. At the time of induction hemin (40 mg/L) was also added to the medium. Twenty hours after induction the cells were harvested. Isolation and purification of the deuterated KatGs was carried out as described previously for the nondeuterated sample.[32]

Enzyme and Protein Determination. Catalase activity was determined by the method of Rørth and Jensen[33] in a Gilson oxygraph equipped with a Clark electrode. One unit of catalase is defined as the amount that decomposes 1 μmol of H_2O_2 in 1 min in a 60 μM H_2O_2 solution at pH 7.0 and 37 °C. Peroxidase activity was determined spectrophotometrically using ABTS (2,2′-azinobis(3-ethlybenzothiazolinesulfonic acid)) ($\epsilon_{405} = 36\,800\ M^{-1}\ cm^{-1}$)[34] or *o*-dianisidine ($\epsilon_{460} = 11\,300\ M^{-1}\ cm^{-1}$)[35] as electron donors. One unit of peroxidase is defined as the amount that decomposes 1 μmol of electron donor in 1 min in a solution of 0.4 mM ABTS or 0.36 mM *o*-dianisidine and 2.5 mM (1 mM for *o*-dianisidine) H_2O_2 at pH 4.5 and 25 °C. The protein was estimated according to the method of Layne.[36] Gel electrophoresis of purified proteins was carried out under denaturing conditions on 8% SDS−polyacrylamide gels.[37,38]

EPR Samples. Native enzyme in 50 mM TRIS−maleate buffer was used for the pH titration experiments, $5.5 \le pH \le 8.5$, on the native (ferric) enzyme. Typically, the Compound I samples were prepared by mixing manually 1 mM native enzyme (50 mM TRIS/maleate buffer, pH 7.0) with an equivolume of 15-fold excess buffered peroxyacetic acid solution (final pH 4.5) directly in the 4 mm EPR tubes kept at 0 °C. The reaction was stopped by rapid immersion of the EPR tube in liquid nitrogen after 7 s. The peroxyacetic acid concentration and mixing time used in these experiments were those providing the highest yield of the radical signal. No detectable differences in the relative contribution of the tyrosyl and tryptophanyl radical signals to the high-field EPR (HF-EPR) spectrum were observed for the wild-type enzyme in samples prepared with shorter or longer mixing times. Using lower excess of peroxyacetic acid (5- or 10-fold excess) resulted in formation of the same EPR signal except for a lower yield, which scaled inversely with conversion of the ferric iron signal. The same spectrum was observed on samples for which the reaction of MtKatG with peroxyacetic acid was made at 20 °C, but a clear lower radical yield was observed as compared to the 0 °C mixing experiments. For the experiments with isoniazid the enzyme was incubated with 5-fold excess INH for 10 min at 20 °C prior to reaction with peroxyacetic acid in the conditions described above (except for shortening the mixing time to 2 s). Spin quantification of the radicals was done using the CcP Compound I signal for estimation of the equivalent [(Fe(IV)═O $Trp_{321}^{\bullet+}$] intermediate in MtKatG and a PSII sample of Tyr_D for the nonexchange-coupled $Trp^\bullet$ and $Tyr^\bullet$ species. The choice of references for spin quantification was done by considering radicals with comparable relaxation properties as well as line shapes.

EPR Spectroscopy. Conventional 9 GHz EPR measurements were performed using a Bruker ER 300 spectrometer with a standard TE_{102} cavity equipped with a liquid helium cryostat (Oxford Instrument) and a microwave frequency counter (Hewlett-Packard 5350B). The home-built high-field EPR spectrometer (95−285 GHz) has been described elsewhere.[39] The absolute error in *g* values was 1×10^{-4}. The relative error in *g* values between any two points of a given spectrum was 5×10^{-5}.

Results

We have previously shown that the EPR spectrum of the *Synechocystis* KatG upon reaction with peroxyacetic acid shows a contribution of three radical species that could only be discerned using a combined approach of multifrequency EPR spectroscopy with deuterium labeling and site-directed mutagenesis.[23,24] The advantageous resolution of the *g*-tensor components in the 285 GHz/10T EPR spectrum of protein-based radicals combined with the changes of the 9 GHz EPR spectrum of such species upon selective perdeuteration of Tyr or Trp residues allowed us to determine the chemical nature of the radicals formed in SyKatG. The same comprehensive approach was used in this work to further investigate MtKatG.

Exchange-Coupled Tryptophan Radical Intermediate in *M. tuberculosis* KatG. The 9 GHz EPR spectrum, recorded at 4 K, of the enzyme upon reaction with peroxyacetic acid is shown in Figure 1 (top, black trace). The spectra of three selected Trp variants on the proximal (W321F) and distal (W107F and W91F) heme sides of the enzyme are also shown for comparison. The 9 GHz EPR spectrum of the wild-type enzyme showed a signal centered at $g \approx 2$ with broad asymmetric wings (Figure 1, top, black trace). The overall width (400 G) and temperature dependence of the broadening (see Figure S1 in Supporting Information) were indicative of at least one organic radical in magnetic interaction with the heme iron. A narrower signal, still detectable at $T \ge 40$ K (peak-to-trough of 20 G and overall width of 75 G; see Figure 2, top), indicated the contribution of an (isolated) radical species to the 9 GHz EPR spectrum. The W107F and W91F variants also showed the 400 G broad (and temperature-dependent) EPR spectra at 4 K (Figure 1, bottom) including the contribution of the narrower signal, readily detected at 60 K (Figure 2, bottom), as in the case of the wild-type enzyme. When hydrogen peroxide was used for the reaction of the catalase-inactive W107F variant, the EPR spectrum was the same as that obtained with peroxyacetic acid as reactant.

The overall width of the MtKatG radical spectrum recorded at 4 K and its temperature dependence was reminiscent of the exchanged-coupled [(Fe(IV)═O $Trp^{\bullet+}$] intermediate in cytochrome *c* peroxidase (see, for example, Figure 2 in ref 40). The UV−vis absorption spectrum of MtKatG upon reaction with peroxyacetic acid (Figure S3 in Supporting Information) showed a very similar pattern to the Fe(IV)═O species of the CcP intermediate (see ref 53 and references therein): the shift of the heme Soret band to 414 nm and α and β bands at 540 and 580 nm. The Trp residue identified in CcP as the unique site for the Trp radical intermediate is conserved in MtKatG; therefore, we constructed and investigated the mutation on the equivalent residue (Trp321) in MtKatG. The 9 GHz EPR spectrum of the W321F variant upon reaction with peroxyacetic acid showed only the narrow radical(s) signal at 4 (Figure 1) and 40 K (Figure 2). The radical species with a 400 G broad EPR signal observed in the wild-type enzyme at 4 K (Figure 1,

(33) Rorth, M.; Jensen, P. K. *Biochim. Biophys. Acta* **1967**, *139*, 171−173.
(34) Childs, R. E.; Bardsley, W. G. *Biochem. J.* **1975**, *145*, 93−103.
(35) Moller, K. M.; Ottolenghi, P. *C. R. Trav. Lab. Carlsberg* **1966**, *35*, 369−389.
(36) Layne, E. *Methods Enzymol.* **1957**, *3*, 447−454.
(37) (a) Laemmli, U. K. *Nature* **1970**, *227*, 680−685. (b) Laemmli, U. K.; Beguin, F.; Gujer-Kellenberger, G. *J. Mol. Biol.* **1970**, *47*, 69−85.
(38) Weber, K.; Pringle, J. R.; Osborn, M. *Methods Enzymol.* **1972**, *26*, 3−27.
(39) Un, S.; Dorlet, P.; Rutherford, A. W. *Appl. Magn. Reson.* **2001**, *21*, 341−361.
(40) Ivancich, A.; Dorlet, P.; Goodin, D. B.; Un, S. *J. Am. Chem. Soc.* **2001**, *123*, 5050−5058.

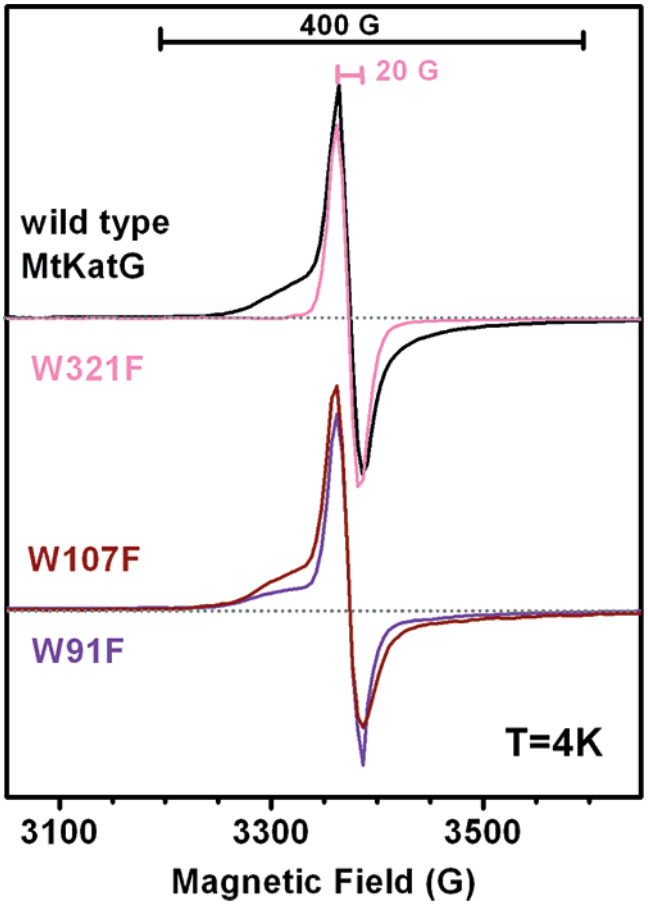

Figure 1. 9 GHz EPR spectra, recorded at 4 K, of the radical intermediate(s) formed in *M. tuberculosis* KatG upon reaction with peroxyacetic acid: the wild-type enzyme spectrum (black trace) is shown together with selected Trp variants of the heme proximal (W321F, magenta trace) and distal (W107F, dark red trace, and W91F, blue trace) sides. Spectra were recorded at 4 K, 3 G modulation frequency, 1 mW microwave power, and 100 kHz modulation frequency.

black trace) was not detected in the W321F variant (Figure 1, magenta trace). Hence, Trp321 appeared to be a good candidate for the exchange-coupled radical site in MtKatG. However, we previously demonstrated that the effect of a single mutation can be misleading for identification of the radical site.[23] Inspection of the crystal structure of MtKatG was used to assess other possible candidates for the site of the exchange-coupled radical. The distal-side Trp107 is close to the heme iron and in H-bonding interaction through a water molecule: the distance between the indole-N of Trp107 and the Fe (4.19[5] or 4.37 Å,[13] depending on the crystal structure) is shorter than that of the CcP radical site (6.81 Å[41]). The EPR signal of a radical forming on Trp107 could be broadened. On this basis we constructed and characterized the W107F variant. Upon reaction with peroxyacetic acid, this variant showed the same 400 G broad EPR signal as the wild-type enzyme at 4 K. Taken together, our findings on the W321F and W107F variants constituted strong evidence for Trp321 being the site for formation of the exchange-coupled radical intermediate in MtKatG.

Comparison of the 4 K EPR spectra of MtKatG wild-type and distal-heme side variants revealed minor but detectable differences on the spectral line shapes. Complementary information on the factors that may contribute to such spectral differences between the proximal Trp321 radical intermediate in MtKatG was obtained with the W91F variant. It was predictable that Trp91 could not to be the site for the exchange-coupled radical since we had previously shown that the 4 K EPR spectrum of the radical species formed on the equivalent residue (Trp106) in SyKatG had an overall width of 75 G with no broadening within the radical line width.[23,24] Not surprisingly, the 4 K EPR spectrum of the MtKatG W91F variant showed the 400 G broad signal (Figure 1, blue trace) as well as the contribution of the narrower signal, as in the case of the wild-type enzyme. However, noticeable differences on the wings of the broad signal were observed. Comparable changes were observed for the W107F variant (Figure 1, red trace). This minor but measurable effect on the line shape of the broad spectra of the variants could reflect differences in the interaction of the heme iron and the Trp radical resulting from the changes on the heme environment. The predominantly axial and non-pH-dependent ferric spectrum of the W107F variant (Figure 4, inset) agreed well with this interpretation if considering that the ferric EPR spectra of native KatGs are very sensitive to mutations on the heme distal side, in particular the distal tryptophan residue.[24,42−44] The ferric EPR spectrum of the W91F variant was also different from the wild-type MtKatG spectrum (Figure 4, inset), and the shape of the broad radical signal was also affected (Figure 1, blue trace). Hence, the W91F variant constituted an excellent case to monitor the influence of small but detectable structural changes in the heme distal side on the exchange-coupled radical signal. However, most importantly, this variant also validated the fact that only the specific mutation of the Trp321 induced the loss of the 400 G broad radical signal (see Figure 1) due to suppression of the site for the exchange-coupled Trp radical in MtKatG. In conclusion, our findings are strong evidence for (a) Trp321 (heme proximal side) and **not** Trp107 (heme distal side) being one of the radical sites in MtKatG and (b) the indirect effect of the W107F and W91F mutations on the 400 G broad EPR signal of the exchange-coupled Trp radical. A similar result was previously reported in the case of CcP variants.[45a,b]

Nonexchange-Coupled Tryptophanyl and Tyrosyl Radical Intermediates: Multifrequency (9−285 GHz) EPR Spectroscopy. We further characterized the 9 GHz EPR spectrum of the narrow radical signal in wild-type MtKatG and Trp variants using experimental conditions to avoid the contribution of the exchange-coupled $Trp^{\bullet+}$ species to the spectra. The wild-type MtKatG spectrum (Figure 2, top) recorded at 60 K was consistent with an isolated organic radical with effective isotropic g value of 2.004, overall width of about 75 G, and peak-to-trough width of 20 G. On the basis of our previous findings in SyKatG, i.e., the contribution of two protein-based radicals to the EPR spectrum,[23] we used the same approach to identify the chemical nature of the radical(s) in MtKatG. When

(41) Bonagura, C. A.; Bhaskar, B.; Shimizu, H.; Li, H.; Sundaramoorthy, M.; McRee, D. E.; Goodin, D. B.; Poulos, T. L. *Biochemistry* **2003**, *42*, 5600−5608.
(42) Jakopitsch, C.; Ivancich, A.; Schmuckenschlager, F.; Wanasinghe, A.; Poltl, G.; Furtmuller, P. G.; Ruker, F.; Obinger, C. *J. Biol. Chem.* **2004**, *279*, 46082−46095.
(43) Carpena, X.; Wiseman, B.; Deemagarn, T.; Herguedas, B.; Ivancich, A.; Singh, R.; Loewen, P. C.; Fita, I. *Biochemistry* **2006**, *45*, 5171−5179.
(44) Deemagarn, T.; Wiseman, B.; Carpena, X.; Ivancich, A.; Fita, I.; Loewen, P. C. *Proteins* **2007**, *66*, 219−228.
(45) (a) Fishel, L. A.; Farnum, M. F.; Mauro, M.; Miller, M. A.; Kraut, J.; Liu, Y.; Tan, X.; Scholes, C. P. **1991**, *30*, 1986−1996. (b) Goodin, D. B.; McRee, D. E. *Biochemistry* **1993**, *32*, 3313−3324.

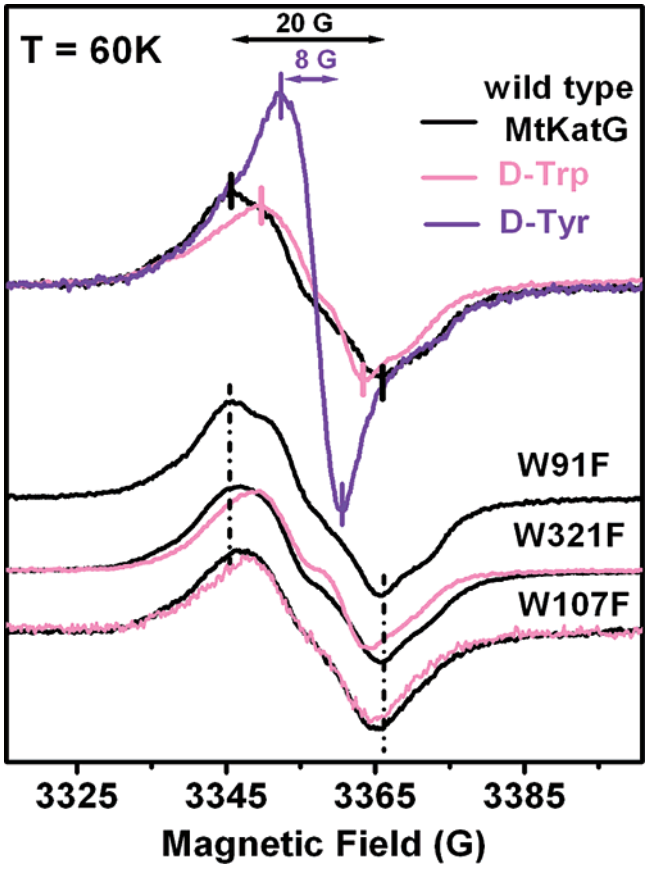

Figure 2. (Top) 9 GHz EPR spectra, recorded at 60 K, of the protein-based radical intermediates in wild-type *M. tuberculosis* KatG (black trace). The spectra of samples containing perdeuterated-Trp (magenta trace) or perdeuterated-Tyr (blue) are superposed. (Bottom) EPR (9 GHz) spectra, recorded at 60 K, of the protein-based radicals of the Trp variants (black traces); the spectra of the corresponding perdeuterated-Trp samples (magenta traces) are superposed. Spectra were recorded at 60 K, 0.5 G modulation frequency, 0.08 mW microwave power, and 100 kHz modulation frequency.

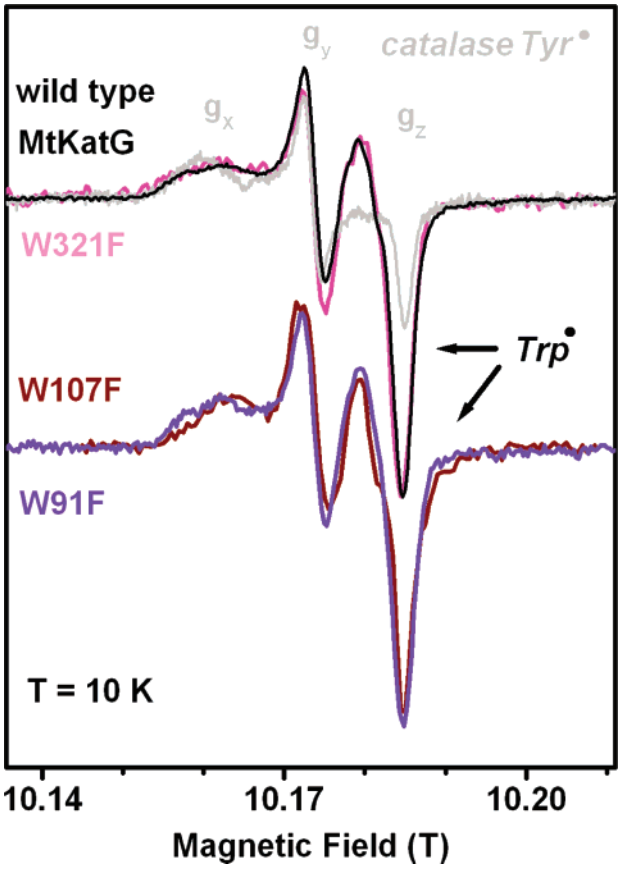

Figure 3. High-field (10 T, 285 GHz) EPR spectra of the protein-based radicals in wild-type (black trace) and selected Trp variants of *M. tuberculosis* KatG. The tyrosyl radical spectrum of the bovine catalase is plotted for comparison (gray trace). Spectra were recorded at 10 K (30 K for the bovine Tyr) using a frequency modulation of 3 kHz and a field modulation of 10 G. The spectra have been aligned to a nominal field to compensate for the calibration in *g* values.

using a perdeuterated-Trp sample the 9 GHz EPR spectrum (recorded at 60 K) of the radical showed the expected changes (narrowing) previously described for the perdeuterated-Trp• signal in SyKatG.[23] The peak-to-trough width of 14 G (Figure 2 top, magenta trace) was totally consistent with the expected predominant Tyr• spectrum upon deuteration of the Trp• species.[23] In the case of the sample for which the tyrosines were perdeuterated, the new central and narrower signal (peak-to-trough width of 8 G) clearly contributing to the spectrum (Figure 2 top, blue trace) was totally consistent with a perdeuterated-Tyr• signal superimposed on the Trp• species.[23] It is worth noting that in MtKatG the perdeuterated Trp and Tyr were not as efficiently incorporated as in the case of the *Synechocytis* enzyme; we estimated 60% incorporation of perdeuterated-Trp and 40% of the perdeuterated-Tyr in the wild-type MtKatG, and yet the changes in the EPR spectrum upon deuteration were clear. Incorporation of perdeuterated-Trp was lower in W107F and within detection error ($\leq$20%) for W91F.

High-frequency EPR (HF-EPR) spectroscopy was applied to obtain complementary information on the *g* tensor of the MtKatG protein-based radicals by means of the enhanced resolution of the *g* anisotropy at higher magnetic fields (see ref 39 and references therein). The design of the high-frequency spectrometer (no cavity) allows us to perform the measurements on the 4 mm EPR tubes used for the commercial 9 GHz EPR spectrometer. Accordingly, the same sample was used for recording both the 285 GHz/10 T (Figure 3) and the 9 GHz/0.3 T EPR (Figure 2) spectra of wild-type and selected Trp variants of MtKatG. The HF-EPR spectrum of MtKatG (Figure 3, black trace) was virtually identical to the previously reported HF-EPR spectrum of SyKatG (see Figure 5 in ref 23), thus showing the contribution of two protein-based radicals, as expected from the deuteration results. The three main components of the high-field spectrum, with observed *g* values of 2.0064(4), 2.0040(5), and 2.0020(8), were consistent with those expected for the intrinsic *g* values of a tyrosyl radical (see ref 23 and references therein). The broad g_x component centered at 2.0064, a fairly low g_x value like the tyrosyl radical in the W191G CcP variant,[40] was indicative of an electropositive and distributed microenvironment to the tyrosyl radical. The width of the g_x component was independent of the frequency of measurement when plotted in a *g*-values scale and thus clearly not due to proton hyperfine couplings. A less anisotropic signal, with an apparent turning point at $g = 2.0026$, contributed with extra intensity to the g_y-g_z region of the Tyr• signal, evident when comparing the HF-EPR spectrum of MtKatG to that of the catalase Tyr•-only spectrum (Figure 3, gray trace). The *g* anisotropy, $\Delta g = g_z - g_x \approx 0.0012$, of the narrower signal in MtKatG agreed well with that expected for a tryptophanyl radical (see ref 46 and

(46) Un, S. *Magn. Reson. Chem.* **2005**, *43*, S229−36.

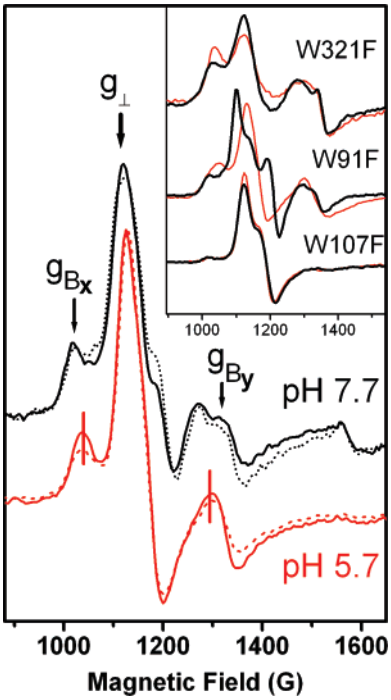

Figure 4. pH dependence of the (4 K) 9 GHz EPR spectra of the resting (native) *M. tuberculosis* KatG. The spectrum shows the contribution of two predominant $S = 5/2$ Fe(III) high-spin forms, one rhombically distorted signal with $g_{Bx} = 6.50$, $g_{By} = 5.10$, and $g_{Bz} = 1.97$ and one axial signal with $g_{A\perp} = 5.90$ and $g_{A||} = 1.99$. Only the expansion of the $g \approx 6$ resonance is shown for clarity; full scan spectra are shown in the Supporting Information (Figure S2). The changes in spectral features happened at pH 7 as in the case of *Synechocystis* enzyme;[23] thus, the spectra at pH 5.7 (solid red trace) and 6.5 (dotted red trace) were identical as well as those at pH 7.7 (solid black trace) and 8.5 (dotted black trace). (Inset) Expansion of the $g = 6$ resonance of the Fe(III) spectra for the Trp variants at pH 5.7 (red traces) and 7.7 (black traces). The ferric spectrum of the W321F variant showed higher contribution of the rhombically distorted signal as compared to the wild-type spectrum, while the W107F was almost axial; no pH dependence was observed for these two variants.

references therein). Interestingly, the ratio of Trp$^\bullet$ to Tyr$^\bullet$ signals contributing to the HF-EPR spectrum in MtKatG (Figure 3) was very similar to that previously observed in SyKatG (see Figure 3 in ref 23). It is of note that while the sample concentration was fine to record a good spectrum of the (isolated) Trp and Tyr radicals (overall breath of 0.05 T when using 285 GHz) we failed to resolve the expected broad signal (0.45 T when using 285 GHz) of the exchange-coupled Trp radical that we previously observed in the case of the CcP Trp radical.[40]

The (60 K) 9 GHz EPR spectrum combined with selective isotope labeling of Tyr and Trp residues and the 285 GHz EPR spectra unequivocally showed formation of two distinct protein-based radicals, Trp$^\bullet$ and Tyr$^\bullet$, in wild-type MtKatG. The HF-EPR spectra of the W107F (dark red trace), W91F (blue trace), and W321F (magenta trace) variants (Figure 3) were also consistent with the contribution of Trp and Tyr radicals to the spectrum, in agreement with the deuteration studies on the same samples (Figure 2). Hence, Trp91 and Trp107 can be ruled out as sites for formation of the Trp$^\bullet$.

Reaction of the Trp Radical Intermediate with Isoniazid in the Peroxidase-Like Cycle. Having demonstrated that we could unequivocally discriminate between the three protein-based radicals (two Trp$^\bullet$ and one Tyr$^\bullet$) formed as intermediates in MtKatG using multifrequency EPR spectroscopy, we pursued the characterization of the putative specific reactivity of these radicals with substrates. In this work, we focused on the enzyme reaction with isoniazid (INH) in an attempt to understand what has been defined as "the activation mechanism" of this prodrug by the enzyme. The conditions in which the reaction of the enzyme with isoniazid was performed turned out to be very important to avoid misinterpretations of the results. Our tests showed that when mixing the enzyme with isoniazid for only few seconds at low temperature no measurable modification on the ferric EPR signal of the native enzyme was detected. In contrast, longer incubation (10 min at 20 °C) resulted in changes in the axial component of the ferric EPR spectrum, as previously reported by Rusnak and co-workers.[47] An evident change in the color of the sample (from red-brownish to red) was observed only when longer incubation times were used. Thus, in all our experiments we have chosen the longer incubation procedure in order to allow proper binding of INH to MtKatG prior to the 2s-mixing with peroxyacetic acid at 0 °C. When adding INH and peroxyacetic acid simultaneously at room temperature an evident competition between (fast) formation of the radical intermediates and the relatively slow access and binding of INH to the enzyme was observed.

Figure 5 (left) shows the 9 GHz EPR spectrum (red trace) of the wild-type enzyme preincubated with a 5-fold excess of INH before the 2s-mixing with a 15-fold excess of peroxyacetic acid. When recorded at 4 K, the broad signal of the exchange-coupled Trp$_{321}^\bullet$ was readily detected, although at variance to the control spectrum (i.e., no INH present; Figure 5 black trace), the narrower component (20 G peak-to-trough) was absent. Comparison of the EPR spectra recorded at 40 K (Figure 5, left, inset) confirmed that while in the control spectrum both (noncoupled) Trp$^\bullet$ and Tyr$^\bullet$ species were detected (black trace), virtually no signal was detected in the enzyme preincubated with INH (red trace). It is of note that the residual signal shown for reference (Figure 5, left, inset, red trace) was detected only when using lower temperature (20 K) and 5 times higher modulation amplitude than for the control sample. It is also of note that the intensity of the ferric signal was twice that of the control spectrum, indicating the cycling back to the native (resting) state of the enzyme after reaction with INH, similar to the usual reaction with substrates in monofunctional peroxidases.

Detection of only the exchange-coupled [(Fe(IV)═O Trp$_{321}^{\bullet+}$] species when incubating the MtKatG ferric enzyme with isoniazid prior to reaction with peroxyacetic acid clearly showed that this intermediate was *not* the species reacting with INH. In order to test these results we analyzed reaction of W321F variant with isoniazid, the rationale of the experiment being that the absence of the exchange-coupled Trp321 intermediate would make no difference for the INH reaction. As in the case of the wild-type enzyme, the Trp$^\bullet$ and Tyr$^\bullet$ species (20 G peak-to-trough width, Figure 5, right, inset, blue trace) were absent when the W321F sample was preincubated with isoniazid prior to mixing with peroxyacetic acid (Figure 5, right, inset, red trace). Instead, 50% of the native enzyme Fe(III) signal was recovered (data not shown) plus a new and very broad spectrum (2000 G overall width) was detected at 4 K (Figure 5, right, red trace). Such a broad spectrum (only detected at $T \leq 30$ K) agreed well

(47) Wengenack, N. L.; Todorovic, S.; Yu, L.; Rusnak, F. *Biochemistry* **1998**, *37*, 15825−15834.

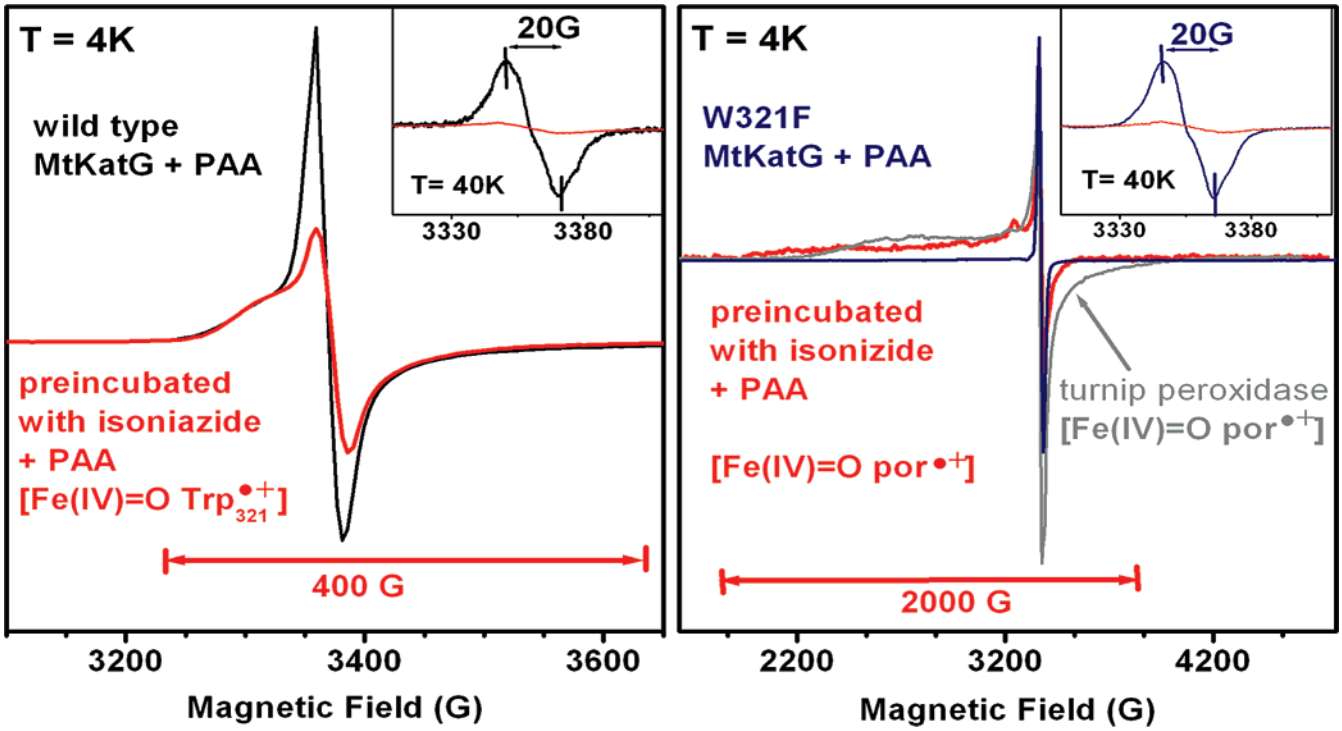

Figure 5. Reaction of wild-type MtKatG (left) and the W321F variant (right) with isoniazid monitored by the 9 GHz EPR spectra of the radical intermediates. The control spectra for the radical intermediates formed in the wild-type enzyme (black trace, left) and the W321F variant (blue trace, right) using peroxyacetic acid (PAA) are the same as those plotted in Figures 1 and 2, respectively. Experimental conditions used are the same as those in Figures 1 and 2. The spectrum of the [Fe(IV)=O Por$^{\bullet+}$] species of turnip peroxidase[49] (gray trace) is plotted for comparison.

with the [Fe(IV)=O Por$^{\bullet+}$] intermediate, well-characterized in mono- and bifunctional peroxidases such as horseradish peroxidase[48] and SyKatG.[23] The spectrum of the [Fe(IV)=O Por$^{\bullet+}$] species formed in turnip peroxidases[49] is shown for comparison (Figure 5, right, gray trace).

Hence, the results observed for the W321F variant with regard reaction with isoniazid strongly support our interpretation that neither [Fe(IV)=O Por$^{\bullet+}$] nor [Fe(IV)=O Trp$_{321}^{\bullet+}$] species are the reactive intermediates with INH. Accordingly, the subsequent Trp$^{\bullet}$ (or Tyr$^{\bullet}$) species should be responsible for the (fast) reaction with isoniazid (see Discussion). It is of note that in the wild-type MtKatG preincubated with INH the yield of [Fe(IV)=O Trp$_{321}^{\bullet+}$] was twice that of the control experiment (see legend in Figure 5, left), while in the case of the W321F variant preincubated with INH, it was possible to accumulate detectable levels of the otherwise short-lived [Fe(IV)=O Por$^{\bullet+}$] intermediate. These observations would support the sequential formation of the radical intermediates (see Figure 6). Moreover, the higher yield of the intermediate preceding the Trp$^{\bullet}$ (or Tyr$^{\bullet}$) species reacting with INH (i.e., [Fe(IV)=O Trp$_{321}^{\bullet+}$] in the wild-type enzyme or [Fe(IV)=O Por$^{\bullet+}$] in the W321F variant) could be explained by a fast reaction of the Trp$^{\bullet}$ (or Tyr$^{\bullet}$) with INH.

Discussion

Our results showed that four radical species are formed in MtKatG: a short-lived [Fe(IV)=O Por$^{\bullet+}$]; the [Fe(IV)=O Trp$_{321}^{\bullet+}$], an exchange-coupled species formed on the heme proximal side Trp as in CcP; a (nonexchange-coupled) Trp radical which at variance with SyKatG does not form on Trp91; and a Tyr radical. In the wild-type enzyme, spin quantification of the radicals resulted in 0.5 spins/heme for the [Fe(IV)=O Trp$_{321}^{\bullet+}$] and 0.3 spins/heme for the signal in which both the Trp$^{\bullet}$ and Tyr$^{\bullet}$ species contributed.

The Exchange-Coupled Trp Radical (Trp321) Intermediate. Our EPR studies on the wild-type MtKatG enzyme and W321F and W107F variants showed that one of the radical intermediates is formed at the same site as in cytochrome *c* peroxidase. While the overall width (and temperature dependence) of the EPR signal of the Trp radical is virtually the same for both CcP and MtKatG, the line shape is different, possibly indicating a difference in the magnetic interaction of the heme iron and the Trp321 radical. Interestingly, minor but possibly relevant differences in the relative position of the proximal-side residues (His270, Asp381, Trp321) and the heme iron are revealed by the crystal structures of CcP and MtKatG. Specifically, comparison of the MtKatG (1SJ2) and CcP (1ZBY) structures shows that the ligation of the imidazole-N of His270 (axial ligand) is 0.37 Å longer in MtKatG (or 0.15 Å if using 2CCA). Also, the distances of the carboxylate of Asp381 to the other imidazole-N of His270 and the indole-N of Trp321 are shorter by 0.24 and 0.14 Å, respectively, in MtKatG as compared to those in CcP. It is of note that the more recent structure by Sachettini and co-workers[13] (2CCA) shows different relative distances of the heme iron, His270, Asp381, and Trp321, as compared to Bertrand and co-workers[5] (1SJ2). The EPR spectrum of the D235E variant of CcP (the equivalent residue to Asp381 in MtKatG) showed a similar spectrum to that of MtKatG.[19,45] The crystal structure of the D235E variant showed a small displacement of the carboxylate and subtle changes in

(48) Schulz, C. E.; Devaney, P. W.; Wrinkler, H.; Debrunner, P. G.; Doan, N.; Chiang, R.; Rutter, R.; Hager, L. P. *FEBS Lett.* **1979**, *103*, 102−105.
(49) Ivancich, A.; Mazza, G.; Desbois, A. *Biochemistry* **2001**, *40*, 6860−6866.

the interaction with both the proximal Trp and the His (heme axial ligand) as compared to the wild-type CcP. This modified geometry of the D235E variant highly resembles the interactions of the axial ligand (His270), Asp389, and Trp321 in MtKatG revealed by the crystal structure.

In previous studies on MtKatG Magliozzo and co-workers[10] reported only a narrow radical EPR signal both for the wild-type and W321F enzymes. These authors reported the 9 GHz EPR spectra recorded at 77 K, making it possible that the exchange-coupled radical was simply not detected in the wild-type enzyme because of unfavorable experimental conditions (see the temperature dependence in Figure S1, Supporting Information). An alternative explanation is that the exchange-coupled radical was not formed in their samples. The fact that the ferric EPR signal reported by Magliozzo and co-workers on their as-isolated enzyme[50] differs from ours (Figure 3) suggests that their enzyme could have a different configuration of the heme pocket that may inhibit formation of the exchange-coupled Trp radical. In our work we observed that only early batches in which the overexpression conditions were not optimal, the enzyme showed different ferric EPR signal and lower catalase activity than our standard samples, and the exchange-coupled Trp radical was not detected or formed only at a defined pH value. Consistent with this observation the catalase activity reported for the W321F variant[10] by Magliozzo and co-workers was 38% of the wild-type enzyme activity,[11] whereas the W321F variant in the current work exhibited comparable catalase activity to the wild-type enzyme. It is of note that our samples have an intact adduct (Trp-Tyr-Met of the heme distal side), as confirmed by the mass spectrometry test on wild-type and W321F samples.

The Trp Radical Intermediate and Reaction with Isoniazid. It was recently proposed that Trp107 and Tyr229 are the primary sites for radical formation in MtKatG.[22] Our findings clearly demonstrate that Trp107 is not the site of the exchange-coupled species or of the other Trp radical intermediate. As previously demonstrated by Ortiz de Montellano and co-workers,[51] a radical-based mechanism should be involved in formation of the cross-link between Trp107 and Tyr229 when the enzyme reacts with H_2O_2 for the first time, but the site for formation of the relatively stable Trp radical species detected by EPR spectroscopy in this work is certainly not Trp107. The EPR characterization of the reaction of wild-type MtKatG and its W321F variant with isoniazid unequivocally showed that the [Fe(IV)═O Por$^{\bullet+}$] and [Fe(IV)═O Trp$_{321}^{\bullet+}$] intermediates are not the species involved in the reaction with the prodrug isoniazid. Accordingly, we concluded that INH should react with the intermediate formed *subsequently* to the [Fe(IV)═O Trp$_{321}^{\bullet+}$] species. From our experiments it is not possible to define whether formation of Trp$^{\bullet}$ precedes the Tyr$^{\bullet}$ species since both contribute to the EPR spectrum obtained by manual mixing. Comparison of the reaction with peroxyacetic acid and hydrogen peroxide on the Y249F variant of SyKatG suggested that Trp$^{\bullet}$ formed first.[42] Moreover, if as suggested by our work, INH has a well-defined binding site, it is tempting to propose that the specific oxidation intermediate for INH should be unique and related to the binding site. We are currently working toward identification of the site for the Trp$^{\bullet}$ intermediate to substantiate our proposal. The fact that reaction with INH does not proceed via the conventional heme-edge reaction of peroxidases implies that the binding site for isoniazid is not the conserved binding site for aromatic substrates in monofunctional peroxidases, as previously proposed on a model based on INH binding to horseradish peroxidase (HRP).[52] The heme distal side in horseradish is far less crowded than that of MtKatG, and binding of isoniazid to a position equivalent to the reported binding site in HRP would require significant changes in the extensive H-bonding network of the heme distal side. Such changes would be reflected by the ferric EPR spectrum (similar to those caused by the W107F variant (see Figure 3)), but this was not the case. Identifying the Trp radical site would definitely help for assessing the putative INH binding site. Although we have not yet identified the Trp (or Tyr) that reacts with INH, one important conclusion from the reactivity of MtKatG with a specific radical site is that the three protein-based radical species (see Figure 6) formed by intramolecular electron transfer, in the absence of substrate, are not side reaction products from random radical migration.

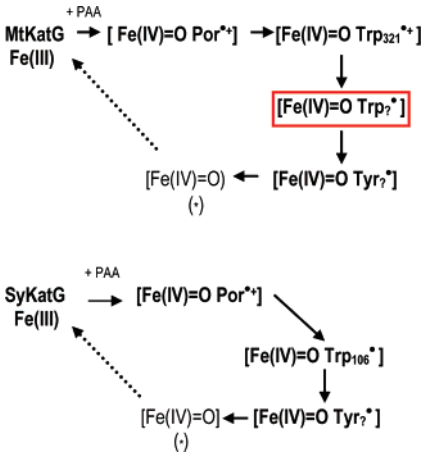

Figure 6. Scheme of the intermediates detected by multifrequency EPR spectroscopy in *M. tuberculosis* and *Synechocystis* KatGs upon reaction with peroxyacetic acid (PAA). The electronic structure of the intermediates included in the scheme is based on direct detection of the EPR spectra with the exception of the [Fe(IV)═O] intermediate (marked with an asterisk); this species is EPR silent (integer spin) but can be inferred from the missing signal when comparing the Fe(III) conversion and yield of the detected intermediates. The Trp radical species marked in the red box is the proposed reactive intermediate with isoniazid.

Proposed Cycle in MtKatG Based on the Intermediates Identified by EPR Spectroscopy: Comparison to the *Synechocystis* Enzyme. The six different oxidation states of MtKatG, including the native ferric (so-called "resting") state, the four radical intermediates that were directly detected and characterized by multifrequency EPR spectroscopy in this work, and the Fe(IV)═O for which the detection was indirect since it is an EPR-silent species, are shown in Figure 6A. The proposed sequential formation of such intermediates is based on the well-characterized case of cytochrome *c* peroxidase as well as our findings with MtKatG variants and the tests of reactivity toward isoniazid. The different intermediates in SyKatG also determined by EPR spectroscopy are shown for comparison (Figure 6B).

(50) Chouchane, S.; Girotto, S.; Kapetanaki, S.; Schelvis, J. P.; Yu, S.; Magliozzo, R. S. *J. Biol. Chem.* **2003**, *278*, 8154−8162.
(51) Ghiladi, R. A.; Knudsen, G. M.; Medzihradszky, K. F.; Ortiz de Montellano, P. R. *J. Biol. Chem.* **2005**, *280*, 22651−22663.
(52) Pierattelli, R.; Banci, L.; Eady, N. A.; Bodiguel, J.; Jones, J. N.; Moody, P. C.; Raven, E. L.; Jamart-Gregoire, B.; Brown, K. A. *J. Biol. Chem.* **2004**, *279*, 39000−39009.

Upon reaction of the native (ferric high-spin oxidation state, Fe(III)) MtKatG with peroxyacetic acid, the [Fe(IV)═O Por$^{•+}$] species is formed. This intermediate is too short lived to be trapped in wild-type MtKatG and evolves to the more stable exchange-coupled [Fe(IV)═O $Trp_{321}^{•+}$] species. In the well-characterized case of CcP it was shown that even when suppressing the Trp radical site (W191F variant) the [Fe(IV)═O Por$^{•+}$] was still relatively short lived and detected only by stopped-flow measurements in the millisecond time scale.[53] Multifrequency EPR spectroscopy characterization of this CcP variant showed formation of a Tyr$^{•}$ species in manual mixing timescale of 15 s[40], clearly subsequent to the [Fe(IV)═O Por$^{•+}$] intermediate observed by stopped-flow spectrophotometry. Similarly, the EPR spectrum of the MtKatG W321F variant showed formation of the (nonexchange-coupled) Trp$^{•}$ and Tyr$^{•}$ species in the manual mixing time range (seconds). Direct evidence for the existence of the [Fe(IV)═O Por$^{•+}$] intermediate was given by the experiments in which the W321F variant was incubated with isoniazid prior to mixing with peroxyacetic acid (Figure 5, right). The detected 2000 G broad EPR signal agreed well with the expected spectrum of an [Fe(IV)═O Por$^{•+}$] species (see Results). In the case of wild-type SyKatG we were able to detect the [Fe(IV)═O Por$^{•+}$] intermediate even when the mixing time was 10 s at 0 °C (see Figure 1B in ref 23), thus showing a longer-lived species likely because the exchange-coupled Trp$^{•+}$ was not stabilized (see Figure 2 in ref 23). The factors determining that the exchange-coupled Trp radical in SyKatG is either not formed or too short lived to be detected remain unclear, although one possible explanation based on the well-documented case of CcP would be that the specific geometry for the interactions of the proximal side residues required to stabilize the Trp radical may not be favorable. A similar situation has been previously reported for the monofunctional ascorbate peroxidase.[54] As shown in the scheme, both MtKatG and SyKatG form a subsequent nonexchange-coupled Trp$^{•}$ (see Figure 6A and B) with the difference between these enzymes being the site of radical formation. Trp106 was shown to be the unique site for the Trp$^{•}$ in SyKatG.[24] The equivalent variant in MtKatG (W91F) exhibited the same EPR spectrum as the wild-type enzyme for the Trp$^{•}$ both at 9 and 285 GHz; thus, it was concluded not to be the radical site in this enzyme. The differences observed in MtKatG and SyKatG reveal that catalase peroxidases are similar to the monofunctional peroxidases in having different radical sites. Such an observation is consistent with the hypothesis that KatGs are ancestors of hydroperoxidases. Further work to identify putative specific substrates for each radical intermediate is in progress.

Comparison to Previously Proposed Intermediates in MtKatG. Previous work from Rusnak and co-workers on MtKatG using 9 GHz EPR and Resonance Raman (RR) spectroscopies characterized the resting (ferric) enzyme,[47,55] binding, and reaction of MtKatG with isoniazid.[15,56,57] A comprehensive work has been published by Magliozzo and co-workers using EPR and RR spectroscopies as well as stopped-flow spectrophotometry to characterize the intermediates of the enzyme and the effect of specific mutations of distal side residues.[9,10,12,21,58−60] Detection of the exchange-coupled Trp radical intermediate formed on the proximal Trp321 in the current work is the main discrepancy to previous work. The previously observed differences of the 9 GHz EPR spectra of the samples prepared by rapid-mix freeze−quench (250 ms) as compared to the manual mixing (10 s) spectra were assigned by Magliozzo and co-workers to a wide doublet Tyr radical as the predominant signal in the millisecond time scale and based on not having detected changes on the Trp-deuterated samples (only the indole protons were deuterated). Our results showed an evident effect of the perdeuteration of Trp on the radical spectrum (Figure 2). Accordingly, an alternative explanation to the previously proposed wide doublet is that a higher proportion of Trp$^{•}$ signal contributed to the spectrum of the freeze−quenched sample as compared to the manual mixing (as previously discussed, see Figure 4 in ref 23). A recent reinterpretation of the 9 GHz EPR spectra together with the 130 GHz EPR spectrum of the radicals by Magliozzo and co-workers[22] acknowledged the contribution of a Trp$^{•}$, although the proposed site for the radical (Trp107) is inconsistent with our findings (see Results).

Ortiz de Montellano and co-workers also extensively characterized the intermediates and reaction of MtKatG with isoniazid by stopped-flow spectrophotometry with a strong emphasis on the role of the post-translational formation of the covalent distal side adduct of Trp107, Tyr229, and Met225.[14,51,61] The proposed catalytic cycle including the reaction with INH (see Scheme 1[14]) relies on the intermediates assigned using the absorption spectra of the enzyme (and variants). Such spectra reflected mostly the changes in electronic structure of the heme iron since the absorption bands for the protein-based radicals are masked. Accordingly, the intermediates proposed by Ghiladi and co-workers differ in detail from those detected by EPR spectroscopy in the current work; in particular, the proposed reaction of the [Fe(IV)═O Por$^{•+}$] intermediate with isoniazid, resulting in an isoniazid radical and a [Fe(III) AA$^{•}$] species, is not supported by our findings. Some of the proposed intermediates, such as the [Fe(III) AA$^{•}$] or the "hypervalent" [Fe(IV)═O Por$^{•+}$AA$^{•}$] species,[14] would be EPR-silent and thus cannot be excluded by our work. A similar mismatch exists for the assignments of the electronic structures of the intermediates based on the stopped-flow UV−vis absorption experiments (for a review, see ref 62) in SyKatG and the radical species detected by EPR spectroscopy (Figure 6 and Discussion in ref 42). Work in progress in our lab aims to specifically combine the complementary information obtained on the heme electronic structure by UV−vis stopped-flow absorption spectrophotometry and the chemical nature of the radicals by multifrequency EPR spectroscopy for the intermediates in MtKatG.

(53) Erman, J. E.; Vitello, L. B.; Mauro, M.; Kraut, J. *Biochemistry* **1989**, *28*, 7992−7995.
(54) Patterson, W. R.; Poulos, T. L.; Goodin, D. B. *Biochemistry* **1995**, *34* (13), 4342−4345.
(55) Lukat-Rodgers, G. S.; Wengenack, N. L.; Rusnak, F.; Rodgers, K. R. *Biochemistry* **2000**, *39*, 9984−9993.
(56) Todorovic, S.; Juranic, N.; Macura, S.; Rusnak, F. *J. Am. Chem. Soc.* **1999**, *121*, 10962−10966.
(57) Wengenack, N.; Rusnak, F. *Biochemistry* **2001**, *40*, 8990−8996.
(58) Chouchane, S.; Lippai, I.; Magliozzo, R. S. *Biochemistry* **2000**, *39*, (32), 9975−9983.
(59) Kapetanaki, S.; Chouchane, S.; Girotto, S.; Yu, S.; Magliozzo, R. S.; Schelvis, J. P. *Biochemistry* **2003**, *42*, 3835−3845.
(60) Zhao, X.; Yu, S.; Magliozzo, R. S. *Biochemistry* **2007**, *46*, 3161−3170.
(61) Ghiladi, R. A.; Medzihradszky, K. F.; Ortiz de Montellano, P. R. *Biochemistry* **2005**, *44*, 15093−15105.
(62) Smulevich, G.; Jakopitsch, C.; Droghetti, E.; Obinger, C. *J. Inorg. Biochem.* **2006**, *100*, 568−585.

Acknowledgment. We thank Sun Un (iBiTec-S, CEA Saclay) for valuable insights and discussions on HF-EPR spectroscopy and Alain Boussac (iBiTec-S, CEA Saclay) for the Tyr radical sample of Photosystem II for spin quantification. R.S. acknowledges a postdoctoral fellowship from CEA Saclay. This work was partially supported by French CNRS and CEA (to A.I.) and grants from the Natural Sciences and Engineering Research Council of Canada (to P.C.L.) and the Canadian Research Chair Program (to P.C.L.).

Supporting Information Available: The temperature dependence ($4\ K \leq T \leq 60\ K$) of the 9 GHz EPR spectrum of the radical intermediates of MtKatG; pH dependence ($5.7 \leq pH \leq 8.5$) of the ferric signal of MtKatG; UV−vis absorption spectra of the wild-type MtKatG and the W107F variant in the ferric (resting) state and upon reaction with peroxyacetic acid. This material is available free of charge via the Internet at http://pubs.acs.org.

JA075108U